J. Biochem. 2009;146(3)343–350
doi:10.1093/jb/mvp076

Fatty Acids Bound to Recombinant Tear Lipocalin and Their Role in Structural Stabilization

Seiichi Tsukamoto, Kazuo Fujiwara and Masamichi Ikeguchi*
Department of Bioinformatics, Soka University, 1-236 Tangi-cho, Hachioji, Tokyo 192-8577, Japan

Received October 27, 2008; accepted May 8, 2009; published online May 26, 2009

A variant of human tear lipocalin was expressed in *Escherichia coli*, and the bound fatty acids were analysed by gas chromatography, mass spectroscopy and nuclear magnetic resonance spectroscopy. Five major fatty acids were identified as hexadecanoic acid (palmitic acid, PA), *cis*-9-hexadecenoic acid (palmitoleic acid), 9,10-methylenehexadecanoic acid, *cis*-11-octadecenoic acid (vaccenic acid) and 11,12-methyleneoctadecanoic acid (lactobacillic acid). The composition of the bound fatty acids was similar to the fatty acid composition of *E. coli* extract, suggesting that the binding affinities are similar for these fatty acids. The urea-induced and thermal-unfolding transitions of the holoprotein (nondelipidated), apoprotein (delipidated) and PA-bound protein were observed by circular dichroism. Holoproteins and PA-bound proteins showed the same stability against urea and heat, and were more stable than apoprotein. These results show that each bound fatty acid stabilizes recombinant tear lipocalin to a similar extent.

Key words: cyclopropane fatty acid, *Escherichia coli*, expression, urea, unfolding.

Abbreviations: HTL, human tear lipocalin; PA, palmitic acid; WT, wild type.

Human tear lipocalin (HTL) is a major lipid-binding protein in human tears where it comprises 15–33% of the total protein content. cDNA cloning and sequencing revealed that HTL comprises 158-amino-acid residues and is a member of the lipocalin family (*1*). The X-ray crystal structure of HTL has been determined at a 1.8 Å resolution and suggests that HTL has a typical lipocalin fold (*2*). HTL is a lipid-binding protein like other members of the lipocalin family, and its physiological role is suggested to remove lipids from the corneal surface (*3*). It was also reported that HTL is important for controlling the viscosity of tears (*4*). However, HTL was found to be produced by a number of other secretory glands such as a lingual glands (von Ebner's gland), and therefore, HTL has another name, von Ebner's gland protein. In such other glands or tissues, HTL must have roles that are different from the role in tear. Furthermore, it was reported that HTL has a cysteine proteinase inhibitor activity (*5*, *6*) and an endonuclease activity (*7*).

Several laboratories have reported on *Escherichia coli* expression systems of recombinant HTL. Holzfeind *et al*. (*8*) expressed a His-tagged HTL using a pQE-70 vector (Qiagen) and M15 as a host. The yield of purified HTL was 15 mg/l of the culture medium, but the article does not describe the bound ligands. Gasymov *et al*. (*9*) inserted the HTL gene into a pET20b vector (Novagen) and then transformed it into *E. coli* BL21(DE3), but we can find no mention of the yield of the purified protein in their papers. They reported that their recombinant HTL was isolated with a bound ligand (*10*), which, when analysed by thin-layer chromatography (TLC), showed that the extracted ligand comigrated with palmitic acid (*10*). Creuzenet and Mangroo (*11*) used pET3d and NovaBlue(lDE3) (both from Novagen) as the expression vector and host strain, respectively. They reported that, of *E. coli* strains, NovaBlue produced the highest level of HTL. The yield of the purified protein was 2 mg from a 4 l culture. It does not appear that the bound substances were examined. Breustedt *et al*. (*2*) fused HTL whose free Cys101 was substituted by Ser to the OmpA signal peptide. The fused protein was secreted into the periplasm of *E. coli*, where processing, folding and the disulfide formation could occur. The protein was purified by streptavidin affinity chromatography using Strep-tag II, which had been fused to the C-terminus. The yield was 1.5–2.5 mg/l of culture. No bound ligand was reported in the crystal structure obtained from this sample (*2*).

Recently, we have constructed an *E. coli* expression system of a HTL mutant to study the folding and unfolding mechanism of HTL (*12*). The wild-type HTL has three Cys residues at positions 61, 101 and 153, and forms a single intramolecular disulfide bond between Cys61 and Cys153. In the mutant protein (C101A), Cys101 was replaced with alanine because free Cys residues frequently cause inter- or intramolecular thiol–disulfide exchange, which complicates the folding reaction.

In this study, we analysed fatty acids bound to the purified C101A and showed that C101A binds unsaturated and cyclopropane fatty acids in addition to saturated fatty acids and that the composition of bound fatty acids was similar to the fatty acid composition of the host cell. We also investigated the effect of bound fatty acids on the conformational stability of C101A.

*To whom correspondence should be addressed. Tel: +81-42-691-9444, Fax: +81-42-691-9312, E-mail: ikeguchi@soka.ac.jp

MATERIALS AND METHODS

Expression and Purification of HTL Protein—The C101A expression vector was constructed as previously described (*12*). The N-terminal His-tagged mutant (C101A) HTL protein was expressed in *E. coli* strain OrigamiB (DE3) (Novagen) transformed by the vector. The transformed *E. coli* was grown in 4 l of the LB medium supplemented with 100 μg/ml ampicillin at 37°C. After the OD_{600nm} reached 0.5, the transformed cells were induced by the addition of 0.1 mM isopropyl β-D-thiogalactopyranoside. The cells were incubated for 4 h, harvested by centrifugation at 4000 × *g* for 15 min, resuspended in a 10 mM sodium phosphate buffer (pH 7.5) and lysed by sonication. The cell lysate was centrifuged at 12,500 × *g* for 15 min, and the supernatant was applied to a $nickel^{2+}$-chelated Sepharose Fast Flow column (75 ml) equilibrated with a 10 mM imidazole–0.5 M NaCl–10 mM sodium phosphate buffer (pH 7.5). C101A was eluted with a linear imidazole gradient (10–200 mM). The eluted fractions were concentrated and then applied to a Sephacryl S-100 gel filtration column (2.6 cm × 80 cm, GE Healthcare Bio-Sciences) equilibrated with 5 mM NH_4HCO_3. The purity of the protein was verified by SDS–PAGE and reverse-phase HPLC, and the purified protein was lyophilized. The yield of the purified protein was 15 mg/l of the culture medium. The disulfide bond formation was confirmed by dithiobis(2-nitrobenzoic acid) titration of the sulfhydryl groups (*13*).

Uniformly ^{15}N-labelled C101A was obtained by growing *E. coli* in the M9 minimal medium with $^{15}NH_4Cl$ as the sole nitrogen source and purified as above.

Delipidation—The purified C101A was delipidated using a modification of the method of Glasgow *et al.* (*14*). The purified C101A was dissolved in a 8 M urea–20 mM sodium phosphate buffer (pH 7.5); the protein concentration was <5 mg/ml. Chloroform–methanol was added at one-half the quantity to the protein solution and mixed thoroughly. The mixture was centrifuged at 3000 × *g* for 10 min, and the aqueous fraction was collected. The extraction by chloroform–methanol was repeated four times. To remove chloroform–methanol completely from the collected protein fraction, the solution was applied to a Sephadex LH-20 gel filtration column (2.6 cm × 20 cm, GE Healthcare Bio-Sciences) equilibrated with a 8 M urea–20 mM sodium phosphate buffer (pH 7.5). The eluted fractions containing C101A were diluted and dialysed with a 20 mM sodium phosphate buffer (pH 7.5). The aggregation of C101A formed by misfolding was removed using a Sephacryl S-100 gel filtration column (2.6 cm × 80 cm, GE Healthcare Bio-Sciences) equilibrated with 5 mM NH_4HCO_3. The eluted fractions containing C101A were lyophilized. Delipidated protein is designated as apoprotein, and non-delipidated protein is designated holoprotein.

Preparation of the Palmitic Acid-Bound C101A Complex—Apo-C101A in a 50 mM sodium phosphate buffer (pH 7.0) was stirred gently and incubated with palmitic acid (high concentration solution in methanol) at 25°C for 12 h. The methanol concentration was <1% to minimize the methanol-induced denaturation of C101A. After 12 h, undissolved palmitic acid was removed by filtering through a sterile 0.22 μm filter. The solution containing C101A was dialysed with 5 mM NH_4HCO_3 and lyophilized. Palmitic acid-bound C101A is designated as PA-C101A.

Identification of Bound Lipids—Lipids were extracted with chloroform and methanol from 5 mg each of apo- and holo-C101A using the method of Glasgow *et al.* (*10*, *14*). The extracted lipids were methylated using a fatty acid methylation kit and a fatty acid methyl ester purification kit (Nacalai Tesque, Inc.). The extracted lipids were analysed using gas chromatography (GC) and GS/mass spectrometry (GC/MS). For quantitative GC analysis, myristic acid equivalent to 80% of the moles of protein was added to the extracted lipids as an internal standard.

GC analysis was performed using a GC-14B combined with a C-R7A Chromatopac (Shimadzu). Chromatographic separation was obtained using a DB-17 capillary column (30 m, 0.32 mm internal diameter, 0.25 μm film thickness, J&W). The oven temperature was kept constant at 180°C.

GC/MS data were collected using an Agilent 6890N gas chromatograph (Agilent Technologies) coupled to a JMS-GCmateII mass spectrometer (JEOL). A methyl silicone capillary column (50 m, 0.25 mm internal dimension, 0.25 μm film thickness, Quadrex) was used for the analysis, and the temperature was changed from 80°C (5 min) to 280°C at a rate of 4°C/min.

Lipids Extraction from E. coli—*E. coli* used for the expression of C101A was grown in the LB medium (50 ml) supplemented with 100 μg/ml ampicillin at 37°C overnight without induction. The cells were harvested by centrifugation at 4000 × *g* for 15 min and then resuspended in a 10 mM sodium phosphate buffer (pH 7.5). An equal amount of chloroform–methanol was added, the suspension was sonicated, the mixture was centrifuged at 3000 × *g* for 10 min and the organic phase was collected. One-half of the extracted lipids was methylated for GC analysis. The other half was evaporated under a stream of N_2 and dissolved in deuterated chloroform for NMR analysis.

NMR Spectroscopy—^1H NMR spectra of extracted lipids were acquired on an ECA-500 NMR spectrometer (JEOL). The chloroform–methanol was evaporated from the extract under a stream of N_2, and the residual was dissolved in deuterated chloroform (Isotec). The spectra were acquired at the ambient temperature.

^1H-^{15}N Heteronuclear Single Quantum Coherence (HSQC) spectra were also acquired on the ECA-500 spectrometer using an automation software GORIN. Samples were prepared at a protein concentration of 1 mM in a 50 mM potassium phosphate buffer including 10% ^2H_2O (pH 6.9). The spectra were acquired at 35°C.

Analytical Ultracentrifugation—Sedimentation equilibrium experiments were performed using an XL-A analytical ultracentrifuge (Beckman) at 25°C. The An-60 Ti rotor and a six-channel charcoal-filled Epon centrepiece were used for each experiment. Before ultracentrifugation, the samples (0.35–0.45 mg/ml) were dialysed against a 0.1 M KCl–50 mM sodium phosphate buffer (pH 7.0) at 4°C. Ultracentrifugation was performed at 32,000 rpm.

Absorbance and CD Measurements—The concentration of C101A was determined from its absorbance spectrum obtained with a UV-2450 UV-VIS spectrophotometer (Shimadzu) and using the extinction coefficient (ε_{280} = 13,000/M/cm), which was determined using the method of Gill and von Hippel (*15*).

CD spectra were recorded on J-720 spectropolarimeter (Jasco) equipped with a Peltier thermostatic cell holder. The path length of the optical cell was 1 mm for the far-UV CD measurement and 10 mm for the near-UV CD measurement.

All experiments were performed in a 50 mM sodium phosphate buffer (pH 7.0).

Urea-Induced Unfolding—The proteins were incubated with varying concentrations of urea from 0 to 8 M at 25°C for 12 h. The urea-induced unfolding transition of C101A was measured using the CD spectrum at 25°C. The final protein concentration was ~0.45 mg/ml at the near-UV region and 0.15 mg/ml at the far-UV region, unless noted otherwise.

Nonlinear least-squares analysis of the equilibrium urea-induced unfolding curve was applied using KaleidaGraph (Synergy Software). The data were analysed by assuming a two-state transition between the native (N) and unfolded (U) states. The observed ellipticity θ_{obs} is represented by the following equation:

$$\theta_{obs} = \frac{\theta_N \exp\{(\Delta G_{NU}^{H_2O} - m_{NU}[\text{urea}])/RT\} + \theta_U}{1 + \exp\{(\Delta G_{NU}^{H_2O} - m_{NU}[\text{urea}])/RT\}}, \quad (1)$$

where θ_N and θ_U are the ellipticity values characteristic of the N and U states, respectively, and are assumed to be a linear function of urea concentration [urea]. The parameters, $\Delta G_{NU}^{H_2O}$ and m_{NU} are the Gibbs free-energy change in water and the cooperativity of unfolding, respectively. The midpoint of the transition, $c_{1/2}$, was calculated by dividing $\Delta G_{NU}^{H_2O}$ by m_{NU}.

Thermal Unfolding and Refolding—Thermal unfolding of C101A was measured by recording the CD signal at 283 nm as a function of temperature every 0.2°C from 20°C to 90°C. In the heating experiments, the temperature was increased at a rate of 2°C/min.

The reversibility of unfolding was examined by scanning the temperature dependence of the CD signal during the cooling process and by comparing it with the heating data.

RESULTS

Identification of Bound Lipids—We found that the recombinant HTL, C101A, which was expressed by *E. coli* OrigamiB, binds various lipids. The GC spectrum of the methylated derivatives of the chloroform–methanol extract showed five major peaks (Fig. 1). The mass and fragmentation pattern in GC/MS analysis suggested that the five major peaks were peaks of methyl esters of (in the order of retention time) palmitic acid (C16:0), palmitoleic acid (C16:1), 9,10-methylenehexadecanoic acid ($_{cyc}$C17:1), vaccenic acid (C18:1) and 11,12-methyleneoctadecanoic acid ($_{cyc}$C19:1). The presence of palmitic acid, palmitoleic acid and vaccenic acid was confirmed by comparing their retention times with those of the methyl ester derivatives of commercially available fatty acids. Because 9,10-methylenehexadecanoic acid and 11,12-methyleneoctadecanoic acid are not available commercially, their existence in the extract was confirmed by their ^{1}H NMR spectra. It is known that the methylene protons of the cyclopropane ring show two characteristic peaks (about –0.3 and 0.6 ppm) (*16*). We found these peaks in the ^{1}H NMR spectrum of the extract (data not shown).

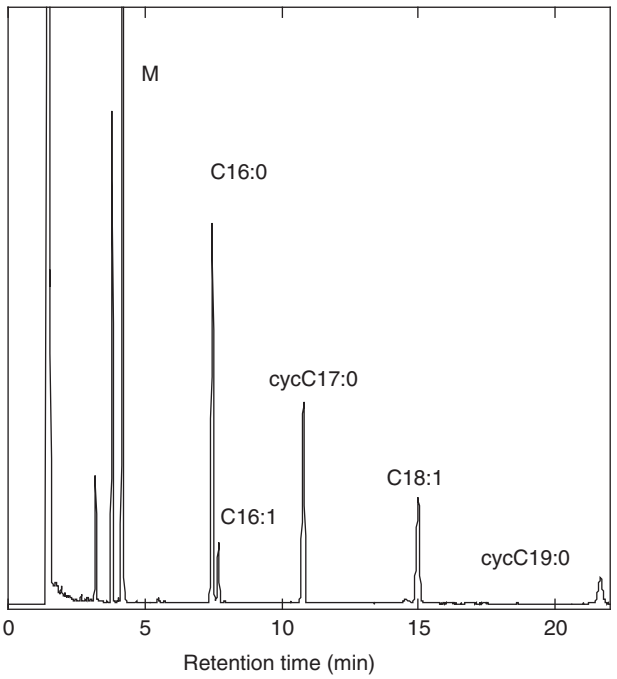

Fig. 1. **Gas chromatogram of the methyl esters of fatty acids extracted from the purified holo-C101A.** The peak marked M is myristic acid added as an internal standard. Peaks labelled C16:0, C16:1, $_{cyc}$C17:1, C18:1 and $_{cyc}$C19:1 were identified as palmitic acid, palmitoleic acid, 9,10-methylenehexadecanoic acid, vaccenic acid and 11,12-methyleneoctadecanoic acid, respectively. Peaks that eluted before M were found in a control experiment in which a buffer solution was used for the extraction and methylation. These peaks probably derive from the fatty acid methylation kit or methyl ester purification kit.

To quantify the bound fatty acids, a known concentration of myristic acid was added to the extraction mixture as an internal standard. Note that the peak of methyl ester of myristic acid in Fig. 1 is the peak of this standard. The amount of each bound fatty acid was calculated from the area of each peak (Table 1). Nearly all (98%) of the purified C101A molecules bound to one of the five fatty acids. Palmitic acid accounted for 43% of the identified fatty acids. We confirmed that the lipids bound to apoprotein accounted for <2% and that palmitic acid bound to PA-C101A.

Because HTL binds a broad array of lipid ligands (*14*), the spectrum of bound fatty acids shown in Table 1 may reflect the fatty acid composition of the *E. coli* host. Therefore, we investigated the composition of fatty acids extracted from *E. coli* OrigamiB (DE3). The result is also shown in Table 1. As expected, the fatty acid

Table 1. **Fatty acid composition of the extract from C101A.**

Fatty acid notation	holo-C101A[a]	apo-C101A[a]	PA-C101A[a]	*E. coli*[b]
C16:0	42	2	94	46
C16:1	7	0	0	1
$_{cyc}$C17:1	25	0	0	28
C18:1	18	0	2	7
$_{cyc}$C19:1	6	0	0	18
Total	98[a]	2[a]	96[a]	

[a]The value of each fatty acid (%) is the molar ratio of each fatty acid to the protein. [b]The value (%) is expressed as the ratio of the amount of fatty acid to the total amount of fatty acids.

composition of *E. coli* OrigamiB (DE3) was similar to that extracted from the purified C101A.

Comparison of Apo- and Holo-C101A Structures—There are conflicting reports about the oligomeric state of HTL (*1*, *11*, *17*, *18*). To address whether apo- and holo-C101A are monomeric or dimeric under our experimental conditions, we performed analytical ultracentrifuge experiments. Holo-, apo- and PA-C101A were all monomeric at pH 7.0 and 25°C (data not shown), showing that at least the C101A mutant with the N-terminal His-tag is monomeric irrespective of the bound ligands.

As shown in Fig. 2, the CD spectrum was similar for apo-C101A and holo-C101A. The CD spectrum of PA-C101A was also similar to holo-C101A. Therefore, the structural change induced by ligand binding was not detected by the CD spectrum. This is inconsistent with the previous result for WT HTL purified from tears (*19*). Gasymov *et al*. (*19*) reported that, in the near-UV region, apo-HTL had a weaker optical activity than did holo-HTL and that the optical activity was restored only partially when stearic acid and cholesterol were added. However, our results showed that the CD spectra of holo-, apo- and PA-C101A are not distinguishable from each other (Fig. 2). The difference from the results of Gasymov *et al*. may reflect the use of different protein samples; our mutant had no free cysteine and had the N-terminal His-tag, whereas the protein used by Gasymov *et al*. was an authentic HTL purified from tears.

Figure 3 shows ^{1}H–^{15}N HSQC spectra of apo-, holo- and PA-C101A. The spectra of holo- and PA-C101A were similar to each other. The number of peaks observed in these spectra (118–131) was fewer than the expected number of peaks, that is, the sum of non-prolyl residues, twice of Asn and Gln residues and tryptophanyl residue (185). Although more peaks were observed in the HSQC spectrum of apo-C101A (163), it is also fewer than the expected value. Missing peaks were probably broadened to a hardly detectable level or overlapped with other detected peaks. The presence of many weak peaks suggested that severe broadening indeed occurred. A possible origin of such broadening is the interchange between the holo- and apo-forms. It is also possible that there are multiple ligand-bound forms and the exchange between them broadens some peaks. The fact that the peak broadening was observed even in apo-C101A suggests that the peak broadening may not be always related to the ligand binding. This poor quality of the

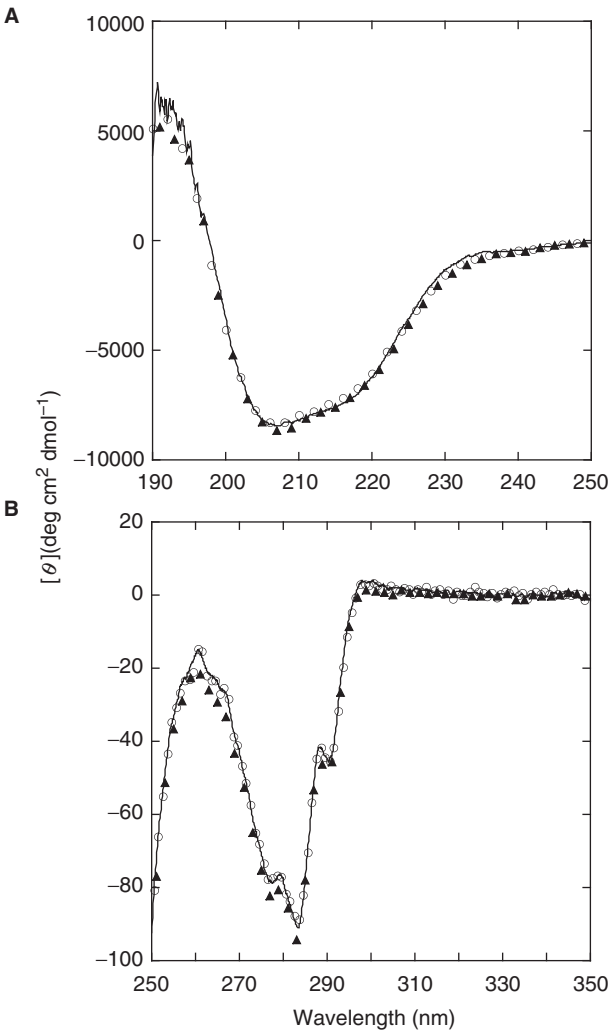

Fig. 2. **The CD spectra of holo- (solid line), apo- (open circle) and PA-C101A (filled trainagle) showing the near-UV CD (A) and far-UV CD (B).**

NMR spectrum prevents us from assigning the peak and discussing the structural change induced by the ligand binding. It is important that, however, the majority of peaks of holo- and PA-C101A (75–80%) overlapped with those of apo-C101A. This suggests that the structures of holo- and PA-C101A are not significantly different from that of apo-C101A, as indicated by CD spectra.

Urea-Induced Unfolding—The urea-induced unfolding transitions of holo-, apo- and PA-C101A were monitored by far- and near-UV CD (Fig. 4). The dependence of the CD values on the urea concentration at both 222 nm and 283 nm for all proteins indicates that both holo- and PA-C101A retained the native conformation up to 4 M, whereas apo-C101A was stable only at a urea concentration <2 M. Above these concentrations, the CD values at both wavelengths showed abrupt increases, indicating that the proteins had unfolded. We confirmed that the unfolding transition was reversible because the data obtained in the refolding experiments coincided with the data of the unfolding experiments. Our data suggest

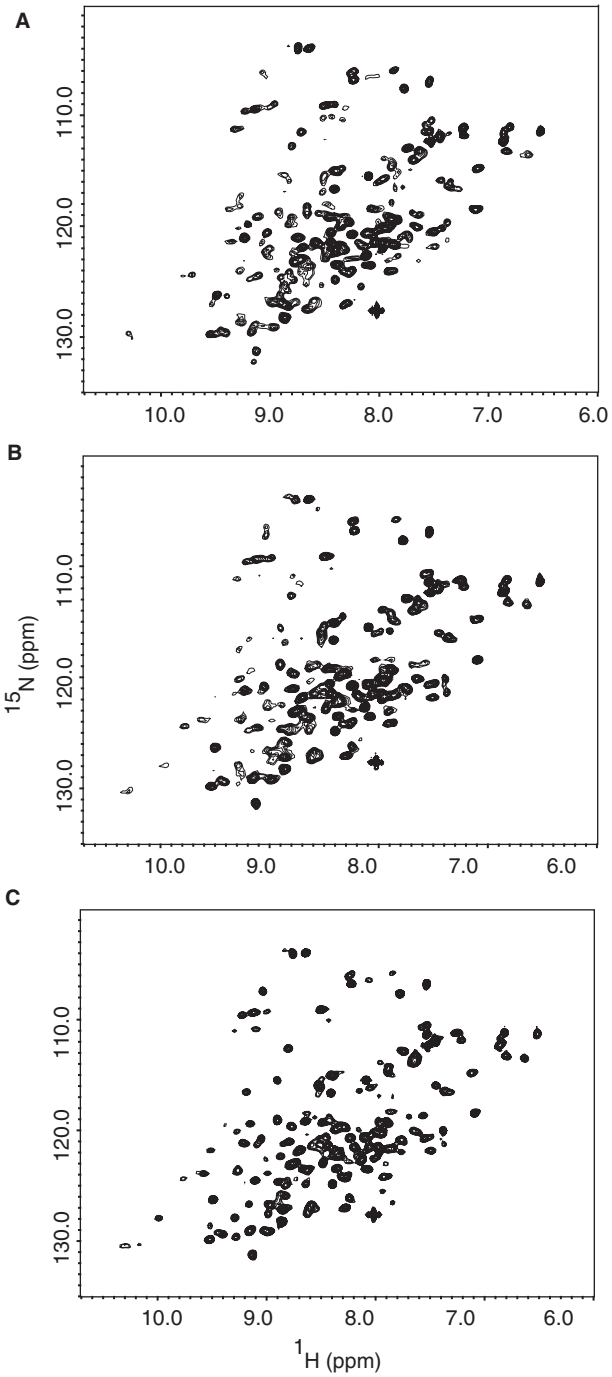

Fig. 3. **HSQC spectra of apo- (A), holo- (B), and PA-C101A (C).** All spectra were acquired at 35°C with the spectral width of 9399 Hz for ^{1}H and 2534 Hz for ^{15}N and the size of the acquired data matrices were 818×256 data points with eight scans per increment. Spectra were resolution enhanced by squared sine-bell functions in both dimensions.

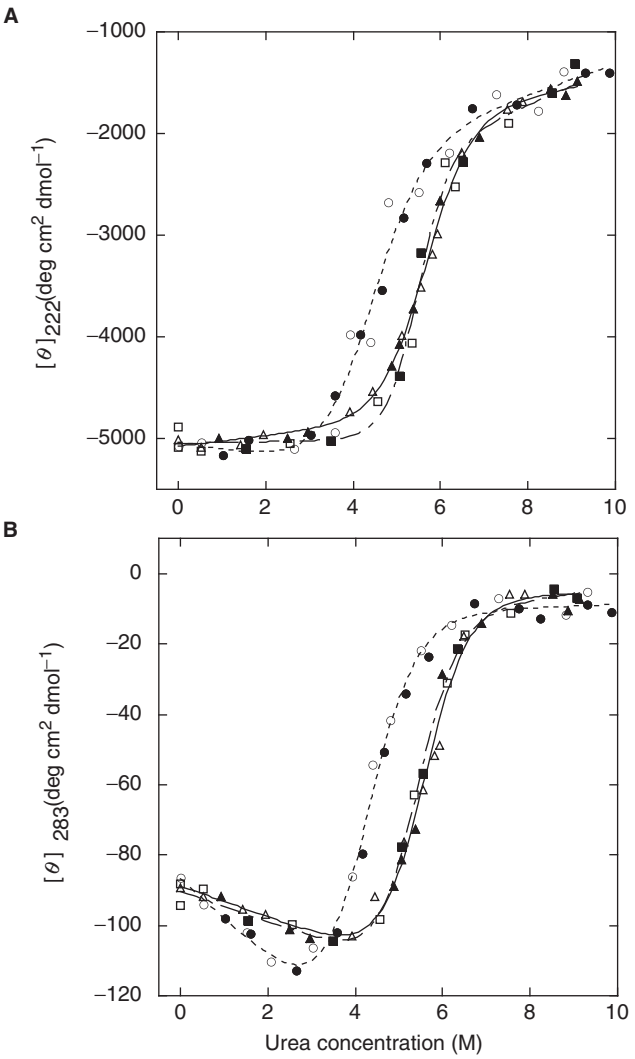

Fig. 4. **The urea-induced unfolding transition of holo- (open triangle, filled triangle), apo- (open circle, filled circle) and PA-C101A (open square, filled square) monitored by CD at 222 nm (A) and 283 nm (B) in a 50 mM phosphate buffer (pH 7.0) at 25°C.** The results of holo-C101A were previously reported (*12*). Open symbols show the data obtained by unfolding of the proteins and the filled symbols show the data obtained by refolding from the unfolded protein. The lines are the best-fit curves based on equation (1).

that the bound fatty acids stabilize the protein conformation. To quantify the stabilization effect, we analysed the urea-induced unfolding transitions by fitting equation (1). The best fitted values of $\Delta G_{NU}^{H_2O}$ and m_{NU} for apo-C101A were 4.50 ± 0.26 kcal/mol and 1.05 ± 0.06 kcal/mol/M, respectively. In contrast, the values of $\Delta G_{NU}^{H_2O}$ and m_{NU} for holo-C101A were 6.64 ± 0.25 kcal/mol and 1.20 ± 0.05 kcal/mol/M, respectively. Similar values were obtained for PA-C101A ($\Delta G_{NU}^{H_2O} = 6.85 \pm 0.49$ kcal/mol and $m_{NU} = 1.25 \pm 0.09$ kcal/mol/M). The similar stabilization by the fatty acid mixture (2.14 ± 0.36 kcal/mol) to that by palmitic acid (2.35 ± 0.55 kcal/mol) suggests that unsaturated fatty acids or cyclopropane fatty acids stabilize C101A to a similar extent as that of palmitic acid.

Thermal Unfolding—The thermal unfolding of holo-, apo- and PA-C101A were monitored by the CD signal at 283 nm (Fig. 5). Because holo- and PA-C101A are very stable at pH 7, we could not observe the entire transition curve within the observed temperature range (<90°C). Therefore, the thermal unfolding transitions

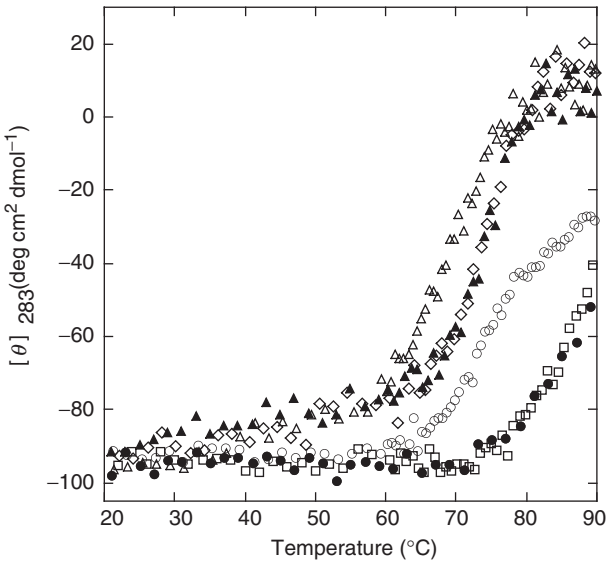

Fig. 5. **Thermal unfolding of holo- (filled triangle, filled circle), apo- (open triangle, open circle) and PA-C101A (open diamond, open square) monitored by CD at 283 nm in a 50 mM citrate buffer (pH 5.0) and in a 50 mM phosphate buffer (pH 7.0).** The triangles and diamond (filled triangle, open triangle and open diamond) show the data at pH 5.0. The circles and square (filled circle, open circle and open square) show the data at pH 7.0.

were observed at pH 5 and 6. At pH 5, a sigmoidal transition curve was observed for both holo- and PA-C101A. However, the cooling experiments revealed that the process was not reversible. Although the thermal unfolding of apo-C101A was partly reversible at pH 7, it was not reversible at a lower pH. Therefore, we did not try to obtain thermodynamic parameters from the thermal unfolding transition. However, our results showed clearly that holo-C101A is as stable as PA-101A and is more stable than apo-C101A.

DISCUSSION

We identified the ligands bound to the purified recombinant HTL. The major ligands were hexadecanoic acid (palmitic acid; C16:0), *cis*-9-hexadecenoic acid (palmitoleic acid, C16:1), 9,10-methylenehexadecanoic acid ($_{cyc}$C17:1), *cis*-11-octadecenoic acid (vaccenic acid, C18:1) and 11,12-methyleneoctadecanoic acid (lactobacillic acid, $_{cyc}$C19:1). Although it is known that HTL binds a wide variety of ligands (*1*, *10*, *14*), this is the first report showing that HTL binds unsaturated fatty acids (C16:1 and C18:1) and cyclopropane fatty acids ($_{cyc}$C17:1 and $_{cyc}$C19:1). The cyclopropane fatty acids are characteristics of bacterial membranes. Several environmental stressors (e.g. temperature, pH and concentration of Mg^{2+}) can change in the fatty acid composition of *E. coli* membranes (*20*, *21*). Only a small amount of cyclopropane fatty acids exists in *E. coli* during the logarithmic growth phase, but their production increases during the stationary phase (*20*, *22*). Because we induced protein synthesis after the $OD_{600\ nm}$ reached 0.5 and collected the membranes 4 h later, the protein was synthesized from the logarithmic growth phase to the stationary phase. The fatty acid composition of the *E. coli* host was analysed after an overnight culture, and the fatty acid composition of *E. coli* shown in Table 1 reflects the composition of the stationary phase. The similarity in the composition between the C101A-bound fatty acids and the fatty acids extracted from the *E. coli* host indicates that the C101A-bound fatty acid reflects the concentrations of the fatty acids in the cell. The C101A-bound fatty acid composition should be affected by both the concentration in the cell and the affinity of C101A for each fatty acid. However, the dissociation constants of HTL for different fatty acids do not differ markedly (*10*). This is also supported by the observation that the conformational stability was similar for holo-C101A and PA-C101A. Therefore, the composition of fatty acids extracted from overexpressed HTL is proportional to the fatty acid concentration in the cell when the protein is synthesized. The percentages of palmitoleic acid and vaccenic acid were greater in C101A-bound fatty acids than in the extracted fatty acids, whereas the percentages of $_{cyc}$C17:1 and $_{cyc}$C19:1 were lower in C101A-bound fatty acids than in the extracted fatty acids (Table 1). This is associated with the observation that C101A synthesis continued from the logarithmic growth phase to the stationary phase. Because palmitoleic acid and vaccenic acid are precursors of $_{cyc}$C17:1 and $_{cyc}$C19:1, respectively, the concentrations of these unsaturated fatty acids should be high during the logarithmic growth phase. It is reasonable to conclude that the protein synthesized during the growth phase binds unsaturated fatty acids and that the protein synthesized during the stationary phase binds cyclopropane fatty acids.

Gasymov *et al*. (*10*) expressed recombinant and mutant HTLs in *E. coli* and analysed the bound ligands. They detected a lipid that comigrated with palmitic acid in TLC. Because the procedure of cultivation was not described in detail, it is difficult to compare their result with ours.

Lowe *et al*. (*23*) investigated the composition of fatty acids bound to intestinal fatty acid-binding protein (IFABP) and liver fatty acid-binding protein (LFABP) expressed in *E. coli*. All fatty acids associated with IFABP were saturated. Palmitic acid and stearic acid comprised 53% and 26%, respectively, of the bound fatty acids. In contrast, LFABP contained C16:1 (10%) and C18:1 (15%) in addition to palmitic acid (42%). No cyclopropane fatty acid was detected in either protein. The absence of bound cyclopropane fatty acid may be explained by its absence in the *E. coli* host during the prestationary phase or by low affinities of IFABP and LFABP for cyclopropane fatty acids.

Generally, proteins are stabilized by the bound ligand if the ligand binds specifically to the protein in its native state. The magnitude of stabilization is a function of the binding constant and the concentration of free ligand (*24*) and can be expressed as follows:

$$\Delta\Delta G = RT\ \ln\left(1+\frac{[L]}{K_d}\right), \qquad (2)$$

where $[L]$ is the concentration of a free ligand and the K_d is the dissociation constant. The magnitude of

Table 2. **Thermodynamic unfolding parameters for C101A.**

	Apo-C101A	Holo-C101A[a]	PA-C101A
$\Delta G_{NU}^{H_2O}$ (kcal/mol)	4.50 ± 0.26	6.64 ± 0.25	6.85 ± 0.49
m_{NU} (kcal/mol/M)	1.05 ± 0.06	1.20 ± 0.05	1.25 ± 0.09
$c_{1/2}$ (M)	4.29 ± 0.12	5.53 ± 0.11	5.46 ± 0.17

[a]From ref. (*12*).

stabilization is estimated most accurately at the midpoint of the unfolding transition. The unfolding midpoint of PA-C101A was 5.46 M urea (Table 2) where the free energy change of unfolding is 0. At the same urea concentration, the unfolding free energy of apo-C101A was calculated as –1.25 kcal/mol, indicating that the stabilization of apoprotein by the bound palmitic acid was 1.25 kcal/mol (Table 2). It is difficult to estimate the concentration of free palmitic acid in the solution used in the unfolding experiments. Assuming that the concentration of free palmitic acid was half of the protein concentration at the unfolding midpoint gives a concentration of ~10 μM. From these estimates and equation (2), the dissociation constant is 1.4 μM. This value is fairly consistent with the value reported previously (*18*), suggesting that the stabilization of C101A by fatty acids is explained by the specific binding to the protein in its native state. The similar stability of holo-C101A and PA-C101A suggests that the dissociation constants for the other bound fatty acids (palmitoleic acid, vaccenic acid, 9,10-methylenehexadecanoic acid and 11,12-methyleneoctadecanoic acid) are similar to that for palmitic acid.

ACKNOWLEDGEMENTS

We thank Dr Hideaki Tsuge (Tokushima Bunri University) for providing the plasmid carrying the WT HTL gene; H. Itoh (Soka University) for help with the delipidation and thin-layer chromatography; Dr Yuri Aoyama (Soka University) for help with the GC analyses; Dr Takashi Niitsu (Soka University) for help with the GC/MS analyses; and Takako Yamashita, Miyuki Satoh, Takahumi Sakamoto and Miwa Ohkouchi for their preliminary work on HTL.

CONFLICT OF INTEREST

None declared.

REFERENCES

1. Redl, B., Holzfeind, P., and Lottspeich, F. (1992) cDNA cloning and sequencing reveals human tear prealbumin to be a member of the lipophilic-ligand carrier protein superfamily. *J. Biol. Chem.* **267**, 20282–20287
2. Breustedt, D.A., Korndorfer, I.P., Redl, B., and Skerra, A. (2005) The 1.8-A crystal structure of human tear lipocalin reveals an extended branched cavity with capacity for multiple ligands. *J. Biol. Chem.* **280**, 484–493
3. Gasymov, O.K., Abduragimov, A.R., Prasher, P., Yusifov, T.N., and Glasgow, B.J. (2005) Tear lipocalin: evidence for a scavenging function to remove lipids from the human corneal surface. *Invest. Ophthalmol. Vis. Sci.* **46**, 3589–3596
4. Gouveia, S.M. and Tiffany, J.M. (2005) Human tear viscosity: an interactive role for proteins and lipids. *Biochim. Biophys. Acta* **1753**, 155–163
5. van't Hof, W., Blankenvoorde, M.F., Veerman, E.C., and Amerongen, A.V. (1997) The salivary lipocalin von Ebner's gland protein is a cysteine proteinase inhibitor. *J. Biol. Chem.* **272**, 1837–1841
6. Wojnar, P., van't Hof, W., Merschak, P., Lechner, M., and Redl, B. (2001) The N-terminal part of recombinant human tear lipocalin/von Ebner's gland protein confers cysteine proteinase inhibition depending on the presence of the entire cystatin-like sequence motifs. *Biol. Chem.* **382**, 1515–1520
7. Yusifov, T.N., Abduragimov, A.R., Narsinh, K., Gasymov, O.K., and Glasgow, B.J. (2008) Tear lipocalin is the major endonuclease in tears. *Mol. Vis.* **14**, 180–188
8. Holzfeind, P., Merschak, P., Rogatsch, H., Culig, Z., Feichtinger, H., Klocker, H., and Redl, B. (1996) Expression of the gene for tear lipocalin/von Ebner's gland protein in human prostate. *FEBS Lett.* **395**, 95–98
9. Gasymov, O.K., Abduragimov, A.R., Yusifov, T.N., and Glasgow, B.J. (1997) Solution structure by site directed tryptophan fluorescence in tear lipocalin. *Biochem. Biophys. Research Commun.* **239**, 191–196
10. Gasymov, O.K., Abduragimov, A.R., Yusifov, T.N., and Glasgow, B.J. (1999) Binding studies of tear lipocalin: the role of the conserved tryptophan in maintaining structure, stability and ligand affinity. *Biochim. Biophys. Acta* **1433**, 307–320
11. Creuzenet, C. and Mangroo, D. (1998) Physico-chemical characterization of human von Ebner gland protein expressed in *Escherichia coli*: implications for its physiological role. *Protein Expr. Purif.* **14**, 254–260
12. Tsukamoto, S., Yamashita, T., Yamada, Y., Fujiwara, K., Maki, K., Kuwajima, K., Matsumura, Y., Kihara, H., Tsuge, H., and Ikeguchi, M. (2009) Non-native alpha-helix formation is not necessary for folding of lipocalin: comparison of burst-phase folding between tear lipocalin and beta-lactoglobulin. *Proteins* **76**, 226–236
13. Riddles, P.W., Blakeley, R.L., and Zerner, B. (1979) Ellman's reagent: 5,5′-dithiobis(2-nitrobenzoic acid)—a reexamination. *Anal. Biochem.* **94**, 75–81
14. Glasgow, B.J., Abduragimov, A.R., Farahbakhsh, Z.T., Faull, K.F., and Hubbell, W.L. (1995) Tear lipocalins bind a broad array of lipid ligands. *Curr. Eye Res.* **14**, 363–372
15. Gill, S.C. and von Hippel, P.H. (1989) Calculation of protein extinction coefficients from amino acid sequence data. *Anal. Biochem.* **182**, 319–326
16. Knothe, G. (2006) NMR characterization of dihydrosterculic acid and its methyl ester. *Lipids* **41**, 393–396
17. Gasymov, O.K., Abduragimov, A.R., Merschak, P., Redl, B., and Glasgow, B.J. (2007) Oligomeric state of lipocalin-1 (LCN1) by multiangle laser light scattering and fluorescence anisotropy decay. *Biochim. Biophys. Acta* **1774**, 1307–1315
18. Redl, B. (2000) Human tear lipocalin. *Biochim. Biophys. Acta* **1482**, 241–248
19. Gasymov, O.K., Abduragimov, A.R., Yusifov, T.N., and Glasgow, B.J. (1998) Structural changes in human tear lipocalins associated with lipid binding. *Biochim. Biophys. Acta* **1386**, 145–156
20. Marr, A.G. and Ingraham, J.L. (1962) Effect of temperature on the composition of fatty acids in *Escherichia coli*. *J. Bacteriol.* **84**, 1260–1267
21. Knivett, V.A. and Cullen, J. (1965) Some factors affecting cyclopropane acid formation in *Escherichia coli*. *Biochem. J.* **96**, 771–776
22. Wang, A.Y. and Cronan, J.E. Jr. (1994) The growth phase-dependent synthesis of cyclopropane fatty acids in *Escherichia coli* is the result of an RpoS(KatF)-dependent

promoter plus enzyme instability. *Mol. Microbiol.* **11**, 1009–1017
23. Lowe, J.B., Sacchettini, J.C., Laposata, M., McQuillan, J.J., and Gordon, J.I. (1987) Expression of rat intestinal fatty acid-binding protein in *Escherichia coli*. Purification and comparison of ligand binding characteristics with that of *Escherichia coli*-derived rat liver fatty acid-binding protein. *J. Biol. Chem.* **262**, 5931–5937
24. Schellman, J.A. (1987) Selective binding and solvent denaturation. *Biopolymers* **26**, 549–559